

## Resonant tunneling through coupled, double-quantum-box nanostructures

Garnett W. Bryant\*

*McDonnell Douglas Research Laboratories, P.O. Box 516, St. Louis, Missouri 63166-0516*

(Received 7 February 1991)

We present calculations of resonant tunneling through coupled, double-quantum-box (CDQB) nanostructures. Resonant tunneling through states confined in individual boxes and resonant tunneling through CDQB states, resonantly coupled between the two boxes, are both important tunneling channels. For weakly coupled boxes separated by a thick barrier, the dominant tunneling channels are the CDQB states. For strongly coupled boxes separated by a thin barrier, CDQB states and individual box states both provide effective tunneling channels. Our results suggest that recent measurements of resonant tunneling in strongly coupled, double-quantum-box nanostructures can be explained as tunneling through states in the box adjacent to the emitter contact.

Reed and co-workers<sup>1-5</sup> and Tarucha *et al.*<sup>6</sup> have used resonant-tunneling spectroscopy to probe electron states confined in isolated, single, quasi-zero-dimensional quantum boxes. The semiconductor nanostructures were fabricated from two-dimensional resonant-tunneling (2DRT) double-barrier structures by laterally confining motion in the contact regions, the two barriers, and the quantum well. The laterally confined contacts are the quantum wires which contact the quantum box. Fine structure superimposed on 2DRT-like current-voltage characteristics was observed for resonant tunneling through small boxes at low temperature ( $T \sim 1-4$  K). This fine structure has been attributed to the discrete density of confined box states.<sup>1-6</sup> Reed and co-workers<sup>2-5</sup> have also used resonant tunneling to probe the confined states in coupled, double-quantum-box (DQB) nanostructures. These structures were fabricated by confining the lateral motion in triple-barrier, double-well structures. Resonant tunneling through coupled boxes also exhibits fine structure in the current-voltage characteristics. Moreover, the fine structure is sharper for tunneling through coupled boxes than for tunneling through single boxes.

To understand the fine structure observed in tunneling through quantum nanostructures, one must know which of the states confined in the nanostructure participate in the resonant tunneling and how resonant tunneling through these states produces fine structure. Reed *et al.*<sup>1</sup> originally suggested that the fine structure they observed in quantum-box resonant tunneling (QBRT) was due to resonant tunneling through box lateral sublevels derived from an *excited* well state. A theory of resonant tunneling through such states,<sup>7</sup> which are broad resonances, predicted observable fine structure only under extreme assumptions about the lateral quantization in the nanostructures.

Recently, careful modeling of band bending in these nanostructures<sup>3-5</sup> has shown that the lateral sublevels derived from the well *ground* state provide the resonant-tunneling channels. A theory of resonant tunneling through these states,<sup>8</sup> which are sharp resonances, pre-

dicts fine structure, for models of Reed's quantum-box nanostructures, which agrees qualitatively with the observed fine structure. When the applied bias brings a confined box state into (out of) resonance with the emitter occupied states, a discrete increase (decrease) in current occurs because a discrete resonant-tunneling channel is opened (closed). A discrete increase in current occurs for increasing bias when the confined state is resonant with the Fermi level. These discrete jumps produce the observed fine structure. Discrete decreases in current with increasing bias should occur when the confined state is resonant with the emitter conduction-band edge. The band-edge crossings occur at higher applied bias than the Fermi-level crossings and so the resonance is broader at the band-edge crossing. In practice, the resonance at band-edge crossing is so broad that the discrete change in current is small and not observable as fine structure in the current-voltage characteristics.

In quantum-box resonant tunneling, the applied bias brings confined states into and out of resonance with the emitter Fermi sea but does not otherwise distort the character of the confined states. The energy-level structure of a CDQB is distorted by the applied bias. For a given applied bias across the CDQB, some of the confined states will be trapped in one box, other confined states will be trapped in the second box. Resonant coupling between the two boxes occurs at applied biases which bring a state in one box into resonance with some state in the second box. In CDQB resonant tunneling (CDQBRT), the applied bias can bring states confined in individual boxes into resonance with the emitter Fermi sea and should produce the fine structure as observed in QBRT. The tunneling current through individual box states in CDQBRT will be smaller than in QBRT because the current must tunnel nonresonantly across one of the boxes. However, when the applied bias distorts the energy-level structure by creating resonantly coupled DQB states, new tunneling channels resonant across the entire structure are opened. If the CDQB states occur at energies resonant with the Fermi sea, then resonant tunneling across the entire structure will occur.

Resonant tunneling through the CDQB states should produce currents much larger than resonant tunneling through states confined to just one of the two boxes. Structure in CDQBRT should be dominated by CDQB tunneling when it occurs. Since the CDQB states occur only for specific applied biases, peaks in the current-voltage characteristic due to CDQB tunneling should be sharp. The width of the CDQB resonant-tunneling peak will be proportional to the width of the CDQB resonance rather than the emitter subband distribution. Effectively, the states confined in the box adjacent to the emitter act as filters. Only emitter states resonant with states in the first box can tunnel resonantly across the *entire* structure. Nakagawa *et al.*<sup>9-11</sup> have studied this filtering effect in two-dimensional double-quantum-well systems. Reed *et al.*<sup>3,4</sup> suggested that filtering by use of a double-box nanostructure would sharpen the fine structure observed in QBRT.

In this paper we present calculations of resonant tunneling through model coupled, double-quantum-box nanostructures to identify qualitatively when structure in the current-voltage characteristic will be produced by tunneling through states localized in individual boxes and when filtering due to tunneling through resonantly coupled DQB states will produce sharpened structure. Calculations are presented as a function of the width of the barrier separating the two boxes to show how the strength of the resonant coupling determines the observable structure. The calculations are shown as a function of emitter subband filling to demonstrate how the resonant tunneling changes as the character of states accessible for tunneling changes. Insight obtained from these results is used to determine which states participate in the CDQB resonant tunneling observed by Reed and co-workers<sup>2-5</sup> and whether filtering is possible in these experiments.

We use the theory previously developed<sup>7,8</sup> for calculations of QBRT to determine the resonant-tunneling current across CDQB nanostructures. We determine the multichannel tunneling current for zero-temperature single-particle resonant tunneling. Tunneling can occur via direct channels, in which the lateral state of the electron is conserved. Tunneling can also occur via indirect channels<sup>7,8</sup> in which the lateral state of the electron changes during tunneling due to scattering from variations in the lateral geometry of the nanostructure. Both types of channels contribute to QBRT and both produce similar fine structure. For our qualitative calculations of CDQBRT, we only consider contributions from direct channels.

We solve the effective-mass Schrödinger equation numerically for the CDQB nanostructures to determine the transmission coefficient for tunneling across the structure. The total current is

$$I = \frac{e}{\pi\hbar} \sum_n \int_{E_{sn}} dE \frac{T(E, n, V) m_s}{\hbar k} [f(E) - f(E + V)],$$

where  $f$  is the occupation factor,  $V$  is the applied bias,  $k$  the wave vector of the incident electron in source subband  $n$  with energy  $E > E_{sn}$ ,  $m_s$  the effective mass in the

source, and  $T$  the transmission coefficient for tunneling in the direct channel starting from source subband  $n$ . The sum is over occupied source subbands. The integral is over the occupied states in each subband. Additional details are given in Ref. 7.

We use simple models for the CDQB band profile to obtain a qualitative understanding of CDQBRT. We assume that the band profile at zero bias is determined by the conduction-band variation. In real structures, charge accumulation makes significant contributions to the band profile and must be included in quantitative calculations.<sup>3-5</sup> We ignore this additional complication in our qualitative model of CDQBRT. Further, we model the applied bias  $V$  (see Fig. 1) as a drop  $V_e$  across the barrier adjacent to the emitter,  $V_c$  across the barrier which couples the two boxes, and  $V_d$  across the barrier adjacent to the drain, with  $V = V_e + V_c + V_d$ .  $V_e$  controls the alignment of energy levels in the upstream box adjacent to the emitter with the emitter states.  $V_c$  aligns levels in the downstream box relative to the levels in the upstream box.  $V_d$  modifies the sharpness of the resonant levels. To qualitatively determine the effects of level alignment we take  $V_d = 0$  and  $V_e = V_c = V/2$ . Other choices for the bias drop change the results quantitatively but do not affect the qualitative insight.

For definiteness, we use GaAs emitter and drain,  $\text{Al}_x\text{Ga}_{1-x}\text{As}$  barriers, and  $\text{In}_{1-y}\text{Ga}_y\text{As}$  boxes as in Ref. 7. The outer barriers are chosen 4 nm wide; the first well, adjacent to the emitter, has a width  $L_1 = 4$  nm; the downstream well has a width  $L_2 = 3.5$  nm. States in the downstream box have higher energy at zero bias than the corresponding states in the upstream box because  $L_1 > L_2$ . In this case, resonant level crossings will occur when a bias is applied. The width of the coupling barrier is chosen to be 10 nm to model CDQBRT in weakly coupled boxes and to be 4 nm to model CDQBRT in strongly coupled boxes. The structure investigated by Reed *et al.* is nominally cylindrically symmetric and the lateral confining potential in each region is effectively parabolic.

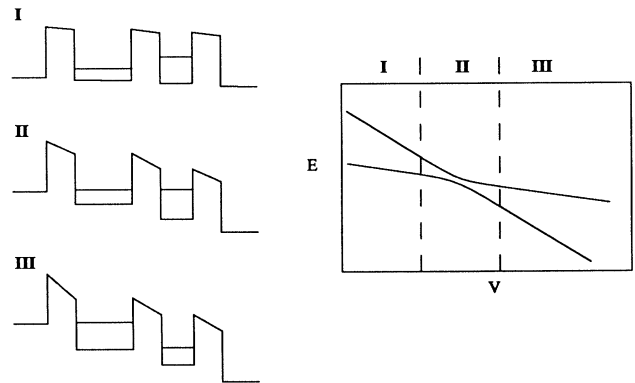


FIG. 1. Energy-level structure of a CDQB structure at low bias (case I), intermediate bias (case II), and high bias (case III). The band profile and ordering of levels trapped in individual boxes is shown for each case.

Successive lateral subbands in each region are equally spaced in energy. The lateral level spacing determines the relative positions of the fine structure in the current due to different direct channels. No other parameters describing the lateral confinement effect the direct tunneling.

The character of CDQBRT is determined by how the occupied emitter states line up with the trapped states as the applied bias is varied. Three cases are possible. At low bias (see Fig. 1, case I) the upstream (wide well) states are at lower energy than the corresponding downstream box states. At some intermediate bias (case II) level crossing of states which can resonantly couple occurs and anticrossings in the level structure happen. At high bias (case III), the ordering of the levels switches and the upstream levels are at higher energy. When the emitter Fermi level  $E_F$  is lower than the energy  $E_r$ , where upstream and downstream trapped levels couple resonantly, the emitter states line up only with trapped states in case III. The tunneling is through the states trapped in individual boxes with the resonant tunneling through upstream states occurring at higher bias than tunneling through the corresponding downstream states. When  $E_F > E_r$  and  $E_r > E_c$  where  $E_c$  is the emitter conduction-band edge, the emitter states line up with trapped states in case II. Tunneling through resonantly coupled DQB states should dominate the CDQBRT. When  $E_c > E_r$ , the emitter states line up only with states in case I. The tunneling is through states trapped in individual boxes with the resonant tunneling through upstream states occurring at lower applied bias than the tunneling through downstream states.

The variation of the current-voltage characteristics with emitter Fermi level  $E_F$  just discussed is clearly exhibited by specific cases. The current-voltage characteristics for resonant tunneling across a weakly coupled DQB with a wide intermediate barrier ( $L_B = 10$  nm) are shown in Figs. 2 and 3. The results are shown for different Fermi levels ( $E_F/\hbar\omega_c$  where  $E_F$  is the emitter Fermi level,  $\hbar\omega_c$  the lateral level spacing in the contacts). The current from the lowest-energy lateral level is shown in Fig. 2. The total current, when more than one lateral subband contributes, is shown in Fig. 3. Because the intermediate barrier is wide, the two boxes are weakly coupled except when there is an on-resonance coupling (level crossing). Thus the CDQB states are narrow resonances.

At low  $E_F$ , tunneling from individual trapped states is clearly seen. A turn on occurs at  $E_F$  crossing and a turn off occurs at  $E_c$  crossing just as in QBRT. The sharpness of the turn on and off result because the applied bias is modeled by drops only across the barriers. Calculations of QBRT (Refs. 8 and 12) show that these sharp structures are broadened substantially, as is actually observed, when more realistic models of the applied bias, which include bias drops across the well, are used. The drop across the well weakens the box resonance and broadens the structure. However, a larger percent of the bias drop will be outside a given well in CDQBRT than in QBRT. Thus structure from tunneling through individual box states should be sharper in CDQBRT than in QBRT.

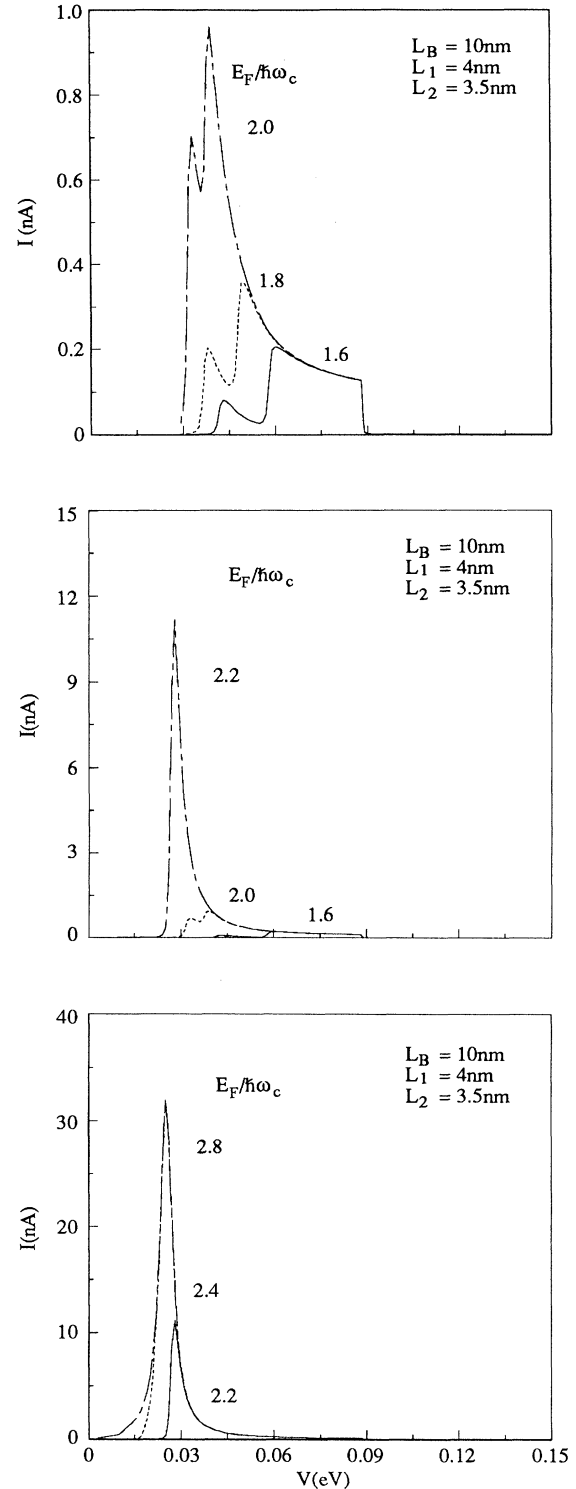


FIG. 2. Current-voltage characteristic of resonant tunneling through a weakly coupled DQB structure. Dependence on emitter Fermi level ( $E_F/\hbar\omega_c$ ) is shown. The upstream well width is 4 nm, downstream well width is 3.5 nm, and the intermediate barrier width is 10 nm. Only the contribution from the lowest-energy lateral subband is shown.

The tunneling current is low because the tunneling is nonresonant across at least one of the boxes. At low  $E_F$  (case III in Fig. 1), resonant tunneling through the upstream state occurs at higher bias than the resonant tunneling through the downstream state. The effective barriers are lower at higher bias, and so resonant tunneling through the upstream state produces a larger current.

As  $E_F$  increases, the CDQB resonance is able to overlap with the emitter states. The structure from resonant tunneling through individual box states begins to merge, revealing the level crossing of the box states. An order-of-magnitude increase in current occurs when the CDQB state can contribute to the tunneling. The narrow peak in the  $I$ - $V$  characteristic reflects the narrow resonance of the CDQB state. The peak position of the CDQB resonance is insensitive to  $E_F/\hbar\omega_c$  and instead is determined by the bias that produces the level crossing. Figure 3

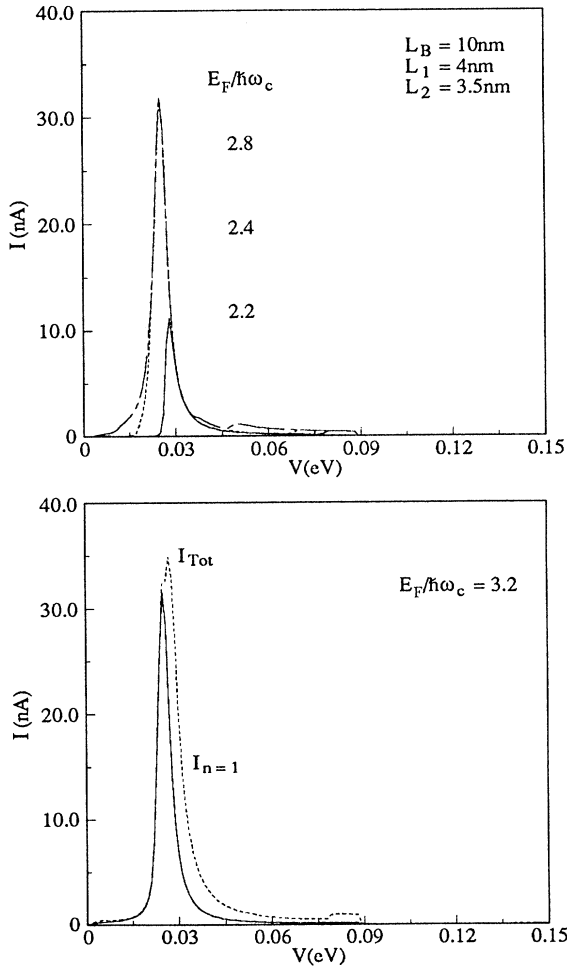


FIG. 3. Current-voltage characteristic of resonant tunneling through a weakly coupled DQB structure. The upper panel shows the total current when two lateral emitter subbands are occupied. The lower panel shows the total current (dashed curve) and the current from the lowest, lateral subband (solid curve) when three lateral subbands are occupied.

shows the  $I$ - $V$  characteristic when several lateral subbands contribute to the tunneling. Since resonant tunneling through CDQB states is dominant, the fine structure due to tunneling through individual states is relatively weak and might not be observable, in practice, for weakly coupled boxes.

CDQBRT for a strongly coupled DQB (thin intermediate barrier,  $L_B = 4$  nm) is shown in Figs. 4 and 5. Tunneling in the lowest-energy lateral channel is shown in Fig. 4 and the total current, when more than one lateral subband contributes, is shown in Fig. 5. The general trends for strongly and weakly coupled boxes are similar. At low  $E_F$ , the fine structure is due to resonant tunneling through individual box states. However, the current is much larger for structures with thin intermediate barriers than for weakly coupled DQB nanostructures.

For strongly coupled boxes, the CDQB resonances are broad resonances. As  $E_F$  increases, the fine structure for tunneling through individual box states merges into a broad structure for tunneling through CDQB states. Tunneling through the CDQB state produces a larger current than tunneling through individual box states. However, the CDQB state tunneling current is not an order of magnitude larger than other tunneling currents as it was for weakly coupled boxes. For weakly coupled DQB nanostructures, the only effective tunneling channels are the CDQB states. For strongly coupled boxes, the intermediate barrier is thin and resonant tunneling across the entire structure is not required to produce a significant current. Figure 5 shows (in contrast to Fig. 3) that tunneling through CDQB states cannot be distinguished clearly from tunneling through individual box states when the boxes are strongly coupled. For example, for  $E_F/\hbar\omega_c = 2.8$  in Fig. 5, the CDQB states produce the broadened structure at low bias, the tunneling through box states produces the structure above 0.03 eV. For  $E_F/\hbar\omega_c = 3.2$ , the lowest-energy CDQB state only produces a background for the structure in the tunneling through other states.

The current-voltage characteristic of a CDQB nanostructure, made from a 6.5-nm-wide upstream well, a 5-nm-wide downstream well, and a thin 3.5-nm-wide intermediate barrier, observed by Reed, Randall, and Luscombe,<sup>4,5</sup> is shown in Fig. 6. A sharp rise in current occurs at  $\sim 800$  meV and six peaks appear in the  $I$ - $V$  characteristics at higher bias. Since the peaks are much sharper than the fine structure observed in QBRT, it is tempting to suggest that these peaks are due to tunneling through CDQB states and that the resulting filtering produces the sharp structure. However, this CDQB nanostructure has a thin barrier. The individual boxes should be strongly coupled and the molecular resonances should be broad and comparable to the structure due to tunneling through individual box states. A consistent interpretation of Reed's observation of CDQBRT can be made in which the peaks in the  $I$ - $V$  characteristics are due primarily to tunneling through states in the upstream box adjacent to the emitter.

Proper modeling<sup>2-5</sup> of the charge redistribution and band bending in quantum-box nanostructures similar to this CDQB nanostructure indicate that the bands are

bent upward near the quantum wells so that the wells are  $\sim 350$  meV higher than the contacts at zero applied bias. This band bending explains why in QBRT an applied bias of 700 mV is needed to bring the box states into resonance with the emitter states. The CDQB nanostructures

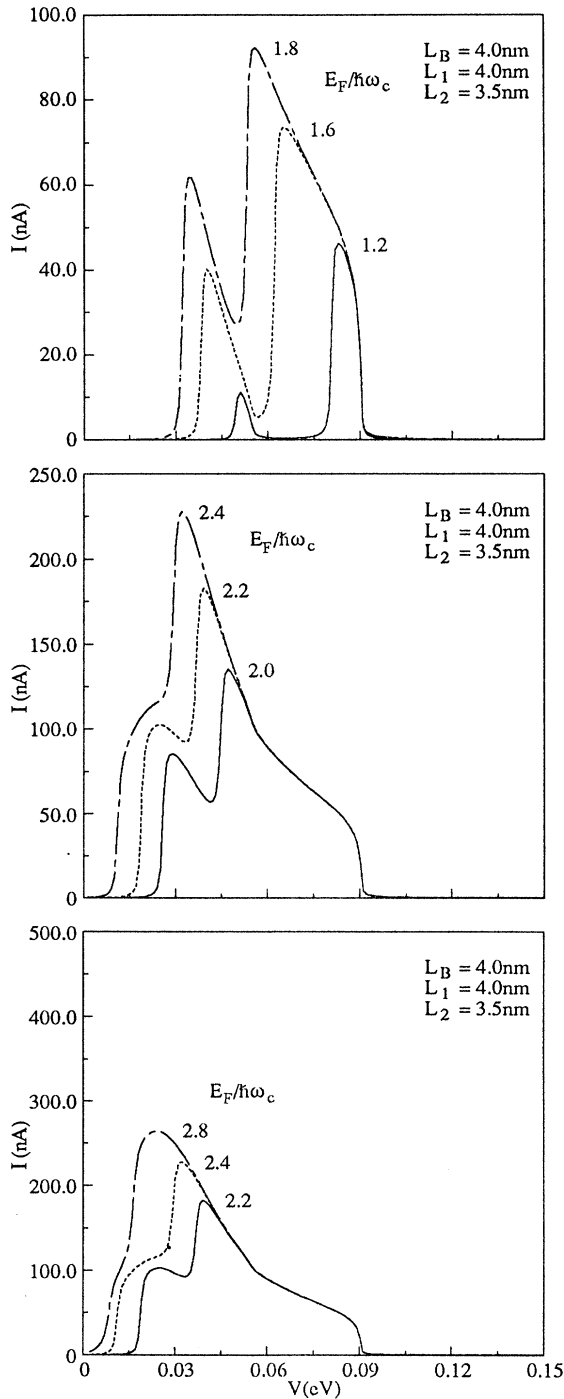


FIG. 4. Current-voltage characteristic of resonant tunneling through a strongly coupled DQB structure ( $L_B = 4$  nm). Only the contribution from the lowest-energy lateral subband is shown.

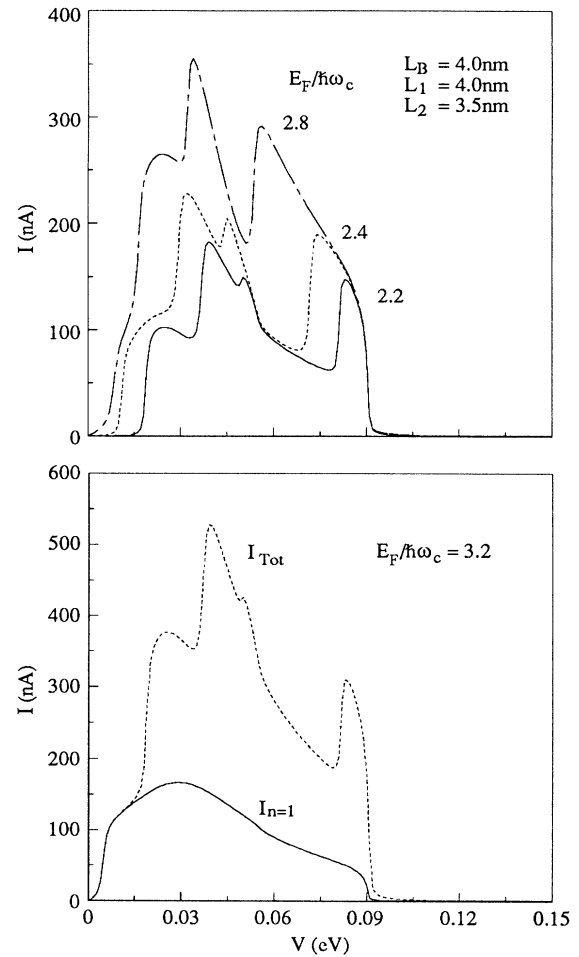


FIG. 5. Current-voltage characteristic of resonant tunneling through a strongly coupled DQB structure. The total currents when two and three lateral emitter subbands are occupied are shown as in Fig. 3.

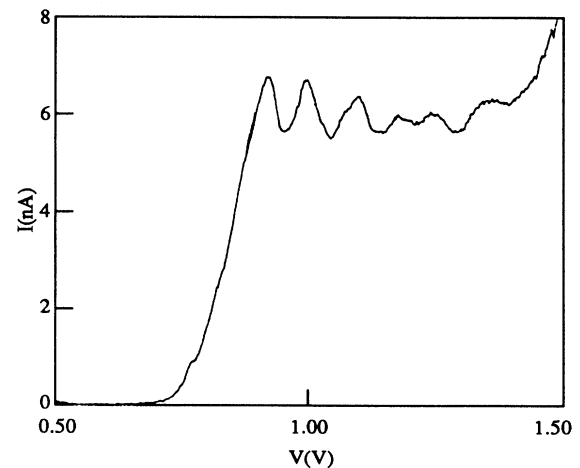


FIG. 6. Current-voltage characteristic of a CDQB structure observed by Reed, Randall, and Luscombe (Refs. 4 and 5) with upstream well width 6.5 nm, downstream well width 5 nm, and intermediate barrier width 3.5 nm.

studied by Reed *et al.* are similar to the boxes that they studied and so a similar band bending should occur near the quantum wells in the CDQB nanostructure.

In a quantum box, approximately half of the bias drop occurs between the emitter and the well. The other half of the drop occurs between the well and the drain. In the CDQB, roughly one-third of the bias drop should occur between the emitter and the upstream box, one-third between the two boxes, and the remaining one-third between the downstream box and the drain. If the band bending at zero bias shifts the wells higher in energy by  $\sim 300$  meV, then states in the downstream well should be in resonance with the emitter for applied bias  $V \gtrsim 450$  mV. States in the upstream well will be resonant with the emitter states for  $V \gtrsim 900$  mV. Thus resonant tunneling occurs when the boxes are aligned as in case III of Fig. 1. As shown in Figs. 2 and 4, tunneling through the downstream states should be much weaker than tunneling through the upstream states. The upstream box is a more effective barrier to resonant transport through the downstream box than the downstream box is to resonant transport through the upstream box because the upstream box is at higher energy. In addition, the effective barrier provided by the band bending is still present for resonant tunneling through the downstream states but is much less significant at higher applied bias for resonant tunneling through the upstream states. As seen in Fig. 6, negligible current exists for  $V \lesssim 900$  mV, as expected for tunneling through the downstream states. The peaks observed above 900 mV result from resonant tunneling through the upstream states.

Resonant tunneling through states trapped in the upstream box produces peaks at the biases for  $E_F$  crossings of the individual box states. Reed, Randall, and Luscombe<sup>4,5</sup> estimate that five emitter lateral subbands are occupied in this structure. Thus direct channels should produce five peaks in the tunneling current. Six peaks are observed. The additional peak may be due to indirect channels or lateral states derived from an excited well state.<sup>5</sup> The peaks are separated in bias by 75, 100,

75, 65, and 125 mV. In a model where one-third of the bias drop is from the emitter to the upstream box, these splittings imply that the level splittings for successive lateral levels are 25, 33, 25, 22, and 42 mV. Although the splittings are irregular, they are consistent with the estimates made for lateral level splittings in quantum-box nanostructures.

The structure at  $E_F$  crossings seen in Fig. 6 for CDQBRT is much sharper than the fine structure at  $E_F$  crossings in QBRT. As mentioned before, sharp peaks in QBRT at the turn on at  $E_F$  crossing occur when the bias drop occurs outside the well but are broadened, as in real systems, substantially when some of the bias drop occurs in the well. Since a larger fraction of the bias drop occurs outside a particular well in CDQBRT than in QBRT, fine structure in CDQBRT should be sharper than in QBRT even though the fine structure is produced by resonant tunneling through individual box states in both cases.

In conclusion, CDQBRT exhibits structure due to tunneling through individual box states and through resonantly coupled DQB states. When the CDQB's are weakly coupled structures made with a thick intermediate barrier, the CDQB resonances are much more effective tunneling channels than the individual box states are. If both types of tunneling contribute to the CDQBRT, then the tunneling from CDQB resonances will make the dominant contribution. In strongly coupled DQB structures made with thin intermediate barriers, both types of tunneling will provide similar contributions. Experiments done on strongly coupled DQB structures exhibit sharp peaks in the current. Resonant tunneling through upstream box states explains this structure. It is unlikely that tunneling through CDQB resonances produces any of the structure.

This research was conducted under the McDonnell Douglas Corporation Independent Research and Development program. Conversations with M. Reed about his experimental results are greatly appreciated.

\*Present address: Applied Physics Branch, U.S. Army Harry Diamond Laboratories, Adelphi, MD 20783-1197.

<sup>1</sup>M. A. Reed, J. N. Randall, R. J. Aggarwal, R. J. Matyi, T. M. Moore, and A. E. Wetsel, *Phys. Rev. Lett.* **60**, 535 (1988).

<sup>2</sup>J. N. Randall, M. A. Reed, R. J. Matyi, and T. M. Moore, *J. Vac. Sci. Technol. B* **6**, 1861 (1988).

<sup>3</sup>M. A. Reed *et al.*, *Festkörperprobleme: Advances in Solid State Physics* **29**, edited by U. Rössler (Vieweg, Braunschweig, 1989).

<sup>4</sup>M. A. Reed, J. N. Randall, and J. H. Luscombe (unpublished).

<sup>5</sup>M. A. Reed, J. N. Randall, and J. H. Luscombe (unpublished).

<sup>6</sup>S. Tarucha, Y. Hirayama, T. Saku, and T. Kimura, *Phys. Rev. B* **41**, 5459 (1990).

<sup>7</sup>G. W. Bryant, *Phys. Rev. B* **39**, 3145 (1989).

<sup>8</sup>G. W. Bryant, *Phys. Rev. B* (to be published).

<sup>9</sup>T. Nakagawa, H. Imamoto, T. Kojima, and K. Ohta, *Appl. Phys. Lett.* **49**, 73 (1986).

<sup>10</sup>T. Nakagawa, T. Fujita, Y. Matsumoto, T. Kojima, and K. Ohta, *Appl. Phys. Lett.* **51**, 445 (1987).

<sup>11</sup>T. Nakagawa, T. Fujita, Y. Matsumoto, T. Kojima, and K. Ohta, *Jpn. J. Appl. Phys.* **26**, L980 (1987).

<sup>12</sup>G. W. Bryant (unpublished).